

- <sup>1</sup>N. F. Lane and S. Geltman, *Phys. Rev.* **160**, 53 (1967).  
<sup>2</sup>H. Ehrhardt and F. Linder, *Phys. Rev. Letters* **21**, 419 (1968); and private communication.  
<sup>3</sup>A. M. Arthurs and A. Dalgarno, *Proc. Roy. Soc. (London)* **A256**, 540 (1960).  
<sup>4</sup>S. C. Wang, *Phys. Rev.* **31**, 579 (1928).  
<sup>5</sup>D. E. Golden, H. W. Bandel, and J. A. Salerno, *Phys. Rev.* **146**, 40 (1966).  
<sup>6</sup>C. Ramsauer and R. Kollath, *Ann. Physik* **4**, 91 (1929).  
<sup>7</sup>R. W. Crompton and A. I. McIntosh, *Phys. Rev. Letters* **18**, 527 (1967); and private communication.  
<sup>8</sup>R. J. W. Henry and N. F. Lane (to be published).  
<sup>9</sup>A. G. Engelhardt and A. V. Phelps, *Phys. Rev.* **131**, 2115 (1963).  
<sup>10</sup>G. Bekefi and S. C. Brown, *Phys. Rev.* **112**, 159 (1958).

PHYSICAL REVIEW

VOLUME 184, NUMBER 1

5 AUGUST 1969

## Pressure Effects of Foreign Gases on the Absorption Lines of Cesium.

V. The Effects of Xenon and CF<sub>4</sub><sup>†</sup>Shang Yi Ch'en, David E. Gilbert,\* and Domingo K. L. Tan<sup>‡</sup>*Department of Physics, University of Oregon, Eugene, Oregon 97403*

(Received 14 April 1969)

The shift, broadening, and asymmetry of the doublet components of the first member of the Cs principal series produced by various relative densities of Xe up to 47 are described. The shift of 17 other high-member doublets is also reported for Xe up to a relative density (rd) of 5. The effects due to Xe are very similar to those due to Kr. The shift, broadening, and asymmetry curves for Xe, although much more pronounced, have the same qualitative shape as our recently reported curves for Ar and Kr. The observed half-widths of various Cs lines produced by CF<sub>4</sub> are very similar to those produced by Xe, and the red shifts are close to those produced by Kr and Xe.

## I. INTRODUCTION

This paper is the fifth in a series.<sup>1</sup> The experimental details and nomenclature are as reported in the earlier papers except that the spectrograph has been converted to a dual-beam instrument followed by an in-line electronic data processing system that enables the direct recording of the absorption coefficient as a function of wavelength. The Xe and CF<sub>4</sub> used was 99.995 and 99.7% pure, respectively. The relative densities (rd) of Xe were computed from the Beattie-Bridgeman equation.<sup>2</sup> Since the broadening and red shift produced by Xe is greater than that for the other rare gases (the separation of red satellites from the main line is also greater for Xe), these effects in the doublet components are more easily detected. CF<sub>4</sub> was chosen because it is a sizable, spherical molecule which would be expected to act like a heavy rare gas with mass and polarizability between those of Kr and Xe.

## II. RESULTS

## A. Shift of Various Cs Absorption Lines by Xenon

The red shift  $\Delta\nu_m$  of the doublet components of the Cs resonance lines produced by Xe, hereafter

abbreviated as Cs(1)/Xe, is shown in Fig. 1. A low-pressure region enlargement of Fig. 1 is given in curve A of Fig. 2, with scale A for shift. Curve B is for Cs(2)/Xe. An absence of an error flag indicates that the error for that point is smaller than the size of the mark. The difference in shift for the two doublet components was detected as shown, but is negligibly small for rd < 7.

The temperatures of the absorption tube and the corresponding Cs vapor pressures for this and for the other figures are given in the third and fourth columns of Table I.

It is quite evident that the plots for  $\Delta\nu_m$  versus rd are not linear for the low-pressure range. This is also reported by Duperier<sup>3</sup> for his measurement of the shift of the <sup>2</sup>P<sub>3/2</sub> component up to rd 12. Due to the nonlinearity of the curve, it is not really appropriate to give the slope of the curve. The values of the slopes for rd < 1 given in Table I are merely average values.

The general shape of Fig. 1 is similar to that for Cs(1)/Kr as previously reported.<sup>4</sup> Due to the increase in intensity and width of the red satellite when the rd of xenon is increased, the positions of the peaks of the two doublet lines were considerably influenced by the overlapping of the broadened satellites and lines. The separation<sup>5</sup>

TABLE I. Slopes of  $\Delta\nu_m$ -versus-rd curves for various Cs lines. "+" means "and larger values"; "s" means the short-wavelength ( ${}^2P_{3/2}$ ) component; "l" means the long-wavelength ( ${}^2P_{1/2}$ ) component.

Figure No.	Narration	Temperature (°K)	Cs vapor pressure (mm Hg)	Slope of $\Delta\nu_m$ versus rd at low pressure ( $\text{cm}^{-1}/\text{rd}$ )	Slope of second linear region ( $\text{cm}^{-1}/\text{rd}$ )
1 and 2(A)	Cs(1)/Xe	333-367	$2 \times 10^{-5}$ - $3 \times 10^{-4}$	-0.25 (s, l) (rd < 1)	-2.22 (l) (18 < rd < 42)
					<u>Broadening</u> [0.49 (rd < 2) ${}^2P_{1/2}$ ] [0.23 (rd < 1) ${}^2P_{3/2}$ ] ...
2B	Cs(2)/Xe	403-472	$2.5 \times 10^{-3}$ - $6.5 \times 10^{-2}$	-0.65 (s, l) (rd < 1)	
3 and 4	Cs(3)/Xe	493-537	$2 \times 10^{-1}$ - $6.5 \times 10^{-1}$	-1.3 (s) -1.5 (l) (rd < 0.5)	-23.9 (s, l) (rd 2.8-5 +)
3	Cs(4)/Xe	493-538	$2 \times 10^{-1}$ - $6.5 \times 10^{-1}$	-2.3 (s) (rd < 0.5)	-27.8 (s) (rd 1.0-4.5 +)
5	Cs(5)/Xe	524-550	$4 \times 10^{-1}$ - $8 \times 10^{-1}$	-6.2 (s) (rd < 0.2)	-28 (s) (rd 0.35-4.5 +)
	Cs(6)/Xe	524-550	$4 \times 10^{-1}$ - $8 \times 10^{-1}$	-16 (s) (rd < 0.07)	-30.5 (s) (rd 2-5 +)
	Cs(7)/Xe	524-550	$4 \times 10^{-1}$ - $8 \times 10^{-1}$	...	-32 (s) (rd 2-5 +)
	Cs(8)/Xe	524-550	$4 \times 10^{-1}$ - $8 \times 10^{-1}$	...	-33 (s) (rd 1.5-5 +)
	Cs(9)/Xe	524-550	$4 \times 10^{-1}$ - $8 \times 10^{-1}$	...	-33 (s) (rd 0.5-5 +)
	Cs(18)/Xe	524-550	$4 \times 10^{-1}$ - $8 \times 10^{-1}$	...	-34 (s) (rd 0.5-5 +)
					-36 (s) (rd 0.2-0.7 +)

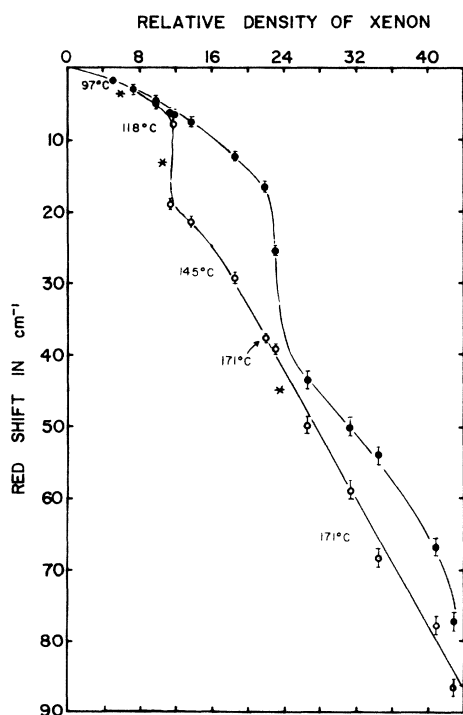


FIG. 1. Red shift of Cs(1)/Xe fine structure components. Closed circle:  ${}^2P_{3/2}$  component; open circle:  ${}^2P_{1/2}$  component. Asterisks mark the boundaries of different temperatures of the absorption tube.

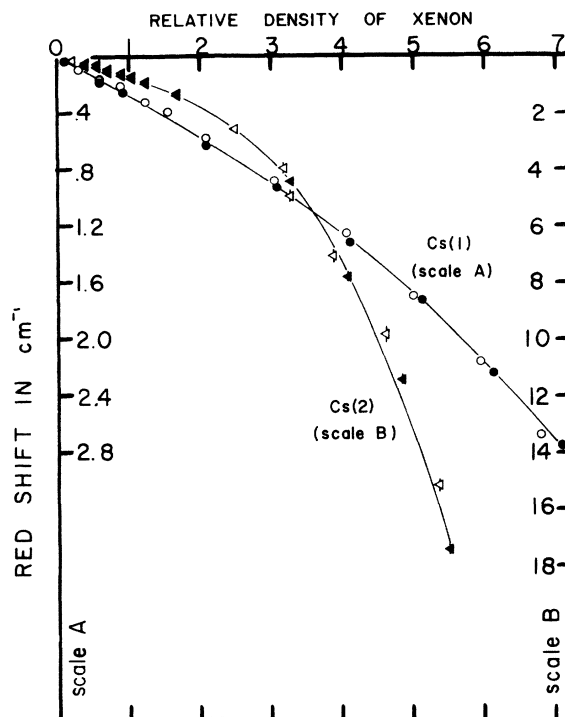


FIG. 2. Red shift of Cs(1)/Xe and Cs(2)/Xe for low-pressure region. Curve A: for Cs(1)/Xe with vertical scale A. Curve B: for Cs(2)/Xe with vertical scale B. Horizontal scale is same for both doublets. Solid circles or solid triangles are for the  ${}^2P_{3/2}$  component; open circles or open triangles are for the  ${}^2P_{1/2}$  component.

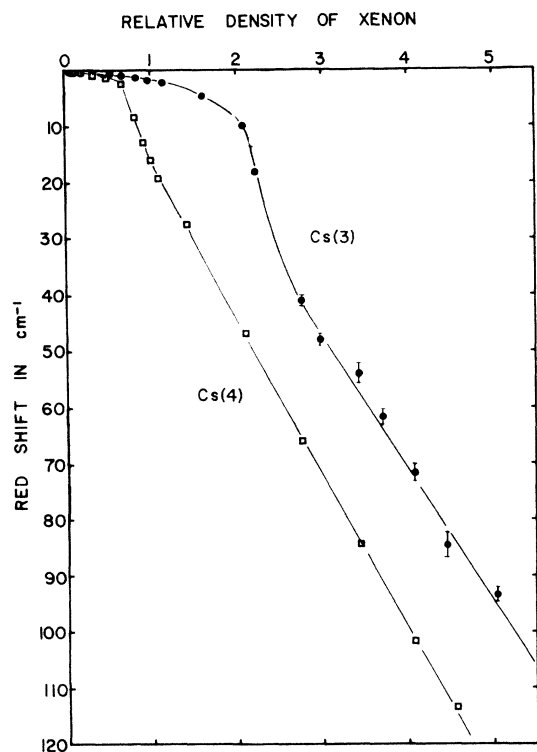


FIG. 3. Red shift of Cs(3)/Xe and Cs(4)/Xe for the  ${}^2P_{3/2}$  component only.

between the  ${}^2P_{1/2}$  component line and its red satellite is  $12.6 \pm 2 \text{ cm}^{-1}$ , and that between the  ${}^2P_{3/2}$  component line and its red satellite is  $33.9 \pm 3 \text{ cm}^{-1}$ . The rapid increase in shift for the  ${}^2P_{3/2}$  component at rd 23–25 and for the  ${}^2P_{1/2}$  component at rd  $\sim 11.5$  is due to the influence of the red satellite. As the rd is increased the red satellite grows, finally becoming more intense than the line. At this point one starts measuring the peak of the completely unresolved satellite rather than the line.

Figure 3 gives the corresponding plots of Cs(3)/Xe and Cs(4)/Xe. A low-pressure enlargement of the curve for Cs(3)/Xe is given in Fig. 4 from which one can see that the curves are nonlinear even for rd  $< 0.5$ . Due to the gradual disappearance of the  ${}^2P_{1/2}$  component with the increase of xenon pressure, it could not be observed with accuracy for rd  $> 1.5$  for Cs(3)/Xe and for rd  $> 0.6$  for Cs(4)/Xe. Measured values within these low-pressure regions reveal that the two fine structure components have nearly the same shifts. The shift of Cs(3)/Xe first increases rather slowly as a function of rd, then at rd  $\sim 0.6$  the shift begins to increase more rapidly with rd. The very rapid increase in shift at rd  $\sim 2.2$  was also due to the influence of the red satellite on the absorption profile just as for Cs(1)/Xe. The faster shift in the second linear region for Cs(3)/Xe was also observed for Cs(4)/Xe. (See Table I.)

It is evident that the suppression of the  ${}^2P_{1/2}$  component becomes more pronounced for heavier gases and for higher member doublets. For Cs(5)/Xe and higher doublets only the shift of the  ${}^2P_{3/2}$  components could be obtained with reasonable accuracy. The shifts of the  ${}^2P_{3/2}$  components of Cs(5), Cs(6), ..., Cs(18) were measured up to rd = 5 and are given in Table I. Figure 5 shows the plots of the shift for low rd only, because for high rd's (up to 5) the plots are essentially a straight line, with a slightly faster increase than linear by about  $-1.8 \text{ cm}^{-1}/\text{rd}$  for the range of rd 1.5–5. (The negative sign indicates a red shift.) For example, the red shift of Cs(9) at rd 4.6 was observed as  $-157 \text{ cm}^{-1}$ . This figure can also be found from Fig. 5, and Table I along with the increment of increase in shift with rd just mentioned.

This slight but definite increase in slope at higher rd (1.5–5) for high-member lines is reported here for the first time. This phenomenon was not observed before in other Cs/rare-gas experiments due to an insufficient number of data points.

The first approximately linear region for Cs(5)/Xe ends at rd = 0.2. The transition region lies between rd = 0.2 and 0.35. The second approximately linear region occurs beyond rd = 0.35. Similarly, the Cs(6)/Xe shift curve has a still

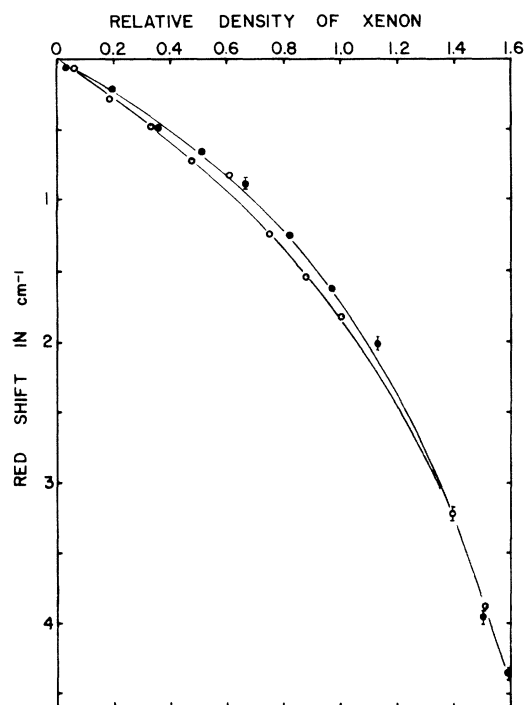


FIG. 4. Low-pressure region enlargement of the shift of Cs(3)/Xe.

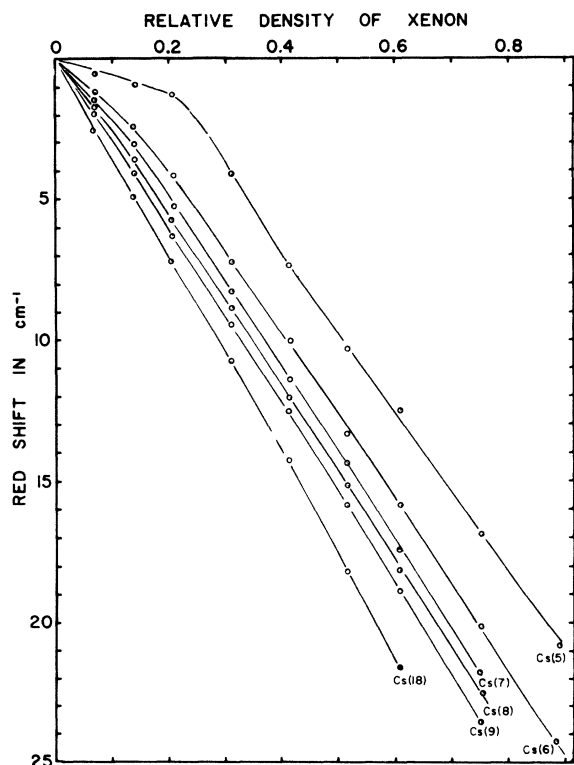


FIG. 5. Shift of the  $^2P_{3/2}$  component of several high-member doublets produced by xenon.

shorter first linear region which ended at rd  $\sim 0.07$ . For Cs(7), (8), and (9)/Xe the first linear region disappears. However, the transition regions are still visible and become shorter and shorter. The curves then show essentially the second approximately linear regions. For still higher-member doublets, it is probably only the second approximately linear regions that one observes. This description indeed corroborates the previous report.<sup>1</sup>

#### B. Broadening Produced by Xenon

The half-width of the doublet components of Cs(1)/Xe is given in Fig. 6. The shape of this figure is very similar to that for Cs(1)/Kr [see Ref. 1(c), p. 44], as one can see from the following comparison. The broadening of both fine structure components is initially the same for both Xe and Kr. For Xe it becomes different, for rd 5–11 [5–10 for Cs(1)/Kr] begins to converge at around rd  $\sim 12$  [10.5 for Cs(1)/Kr], crosses at rd  $\sim 16.5$  [15.5 for Cs(1)/Kr] and finally diverges again in the opposite direction. The  $^2P_{1/2}$  component follows a pronounced S-shaped curve until at rd  $\sim 18$  [15 for Cs(1)/Kr] when it

becomes nearly linear with a little downward bend and with a slope of  $1.1 \text{ cm}^{-1}/\text{rd}$  [0.86 for Cs(1)/Kr]. The  $^2P_{3/2}$  component follows a slight S-shaped curve until at rd  $\sim 22$  [20 for Cs(1)/Kr] when it becomes nearly linear with a little downward bend and with a slope of  $3.5 \text{ cm}^{-1}/\text{rd}$  [1.92  $\text{cm}^{-1}/\text{rd}$  for Cs(1)/Kr]. The broadening by Xe is about 1.8 times stronger than that caused by Kr for the rd range 20–40.

#### C. Asymmetry of Cs(1)/Xe

Figure 7 shows the asymmetry at half-intensity points for the Cs(1)/Xe fine structure lines. The shapes of the curves are very similar to those for Cs(1)/Kr. The asymmetry for the former is stronger than that of the latter by a factor of 1.7, with the  $^2P_{1/2}$  component peaked at rd  $\sim 11$  [7.5 for Cs(1)/Kr] in a narrow rd region of 5–13 [also about 5–13 for Cs(1)/Kr], and with the  $^2P_{3/2}$  component peaking at rd  $\sim 19$  [17 for Cs(1)/Kr] in a narrow rd region of 7–24 [same as for Cs(1)/Kr].

#### D. Effects of $\text{CF}_4$

The shifts of Cs(1)/ $\text{CF}_4$  are shown in Fig. 8. The slopes of the curves for rd  $< 2.5$  ( $T = 34^\circ\text{C}$ ) are 0.29 and  $0.23 \text{ cm}^{-1}/\text{rd}$  for the  $^2P_{1/2}$  and  $^2P_{3/2}$  components, respectively. When the pressure and temperature was increased the reaction of Cs with  $\text{CF}_4$  was greatly accelerated. Consequently, only one pair of readings was obtained

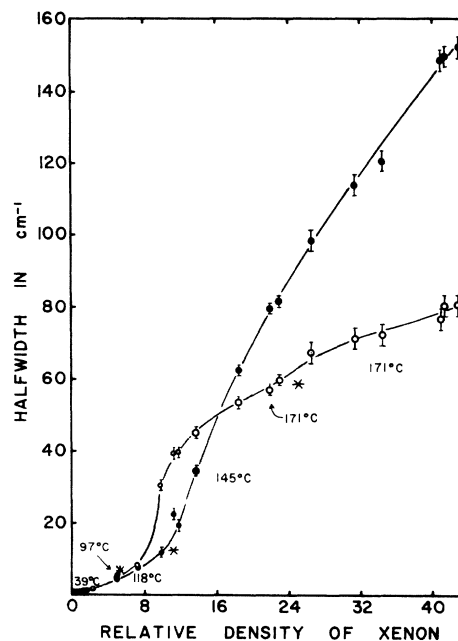


FIG. 6. Half-width of Cs(1)/Xe.

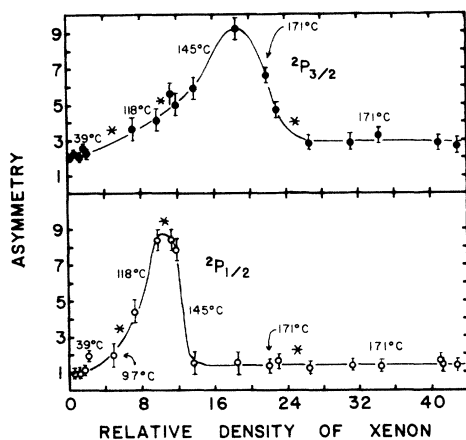


FIG. 7. Asymmetry at half-intensity points for Cs(1)/Xe fine structure lines.

at  $rd = 11.3$ . The  ${}^2P_{1/2}$  component shifts much the same as Cs(1)/Xe or Cs(1)/Kr, while the  ${}^2P_{3/2}$  component shifts close to that of Cs(1)/Kr and Cs(1)/Ar. The half-width for both  ${}^2P_{1/2}$  and  ${}^2P_{3/2}$  components measured from  $rd$  0.04 to 2.32 coincides, within error limits, with the half-widths produced by Xe.

Measurements of the shifts of the Cs high-member doublets by  $CF_4$  were attempted for  $rd = 0.07$  and  $0.172$ . When a straight line was drawn through the data points obtained at these two  $rd$  values in the plot of  $\Delta\nu_m$  versus  $rd$  for each  ${}^2P_{3/2}$  component line of the doublet, the slopes of the lines are  $7 \pm 1$ ,  $9 \pm 1$ ,  $12 \pm 1$ ,  $13 \pm 1$ , and  $14 \pm 1$   $cm^{-1}/rd$  for the 5th through the 9th members of the absorption series, respectively. The shift due to  $CF_4$  is greater than that due to Ar but not quite as great as Kr and Xe.

### III. DISCUSSION

The shift, broadening, and asymmetry observed with Xe are consistent with the results

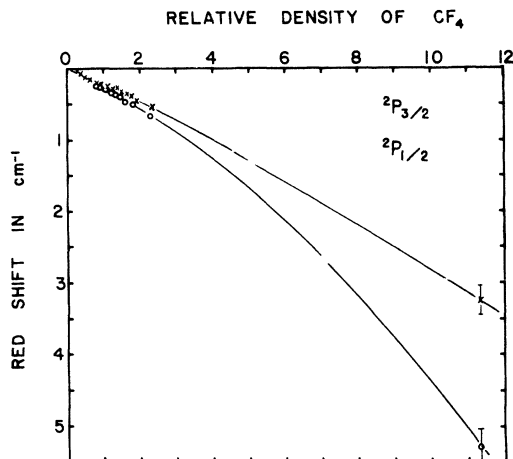


FIG. 8. Shift of Cs(1)/ $CF_4$  fine structure components.

reported for Ar and Kr. As pointed out in Paper III [see Ref. 1(c), p. 44], the results show strongly the insufficiency of considering only the  $R^{-6}$  van der Waals potential. Behmenburg,<sup>6</sup> who extended Lindholm's Theory<sup>7</sup> to include the repulsive  $R^{-12}$  term, was able to explain very beautifully the results of our first four articles. Fiutak<sup>8</sup> calculated quantum mechanically the higher terms in the expansion of the intensity distribution for high  $rd$  and showed also a much closer agreement between our results and theoretical calculations than other present theories. Currently, we have theoretical work underway to obtain an accurate form of the correlation function for an assumed potential difference curve characterized by a few parameters. Preliminary calculations show that the function can oscillate for small correlation time such that the resulting line shape has additional peaks on the line wings that resemble the observed collision induced satellites. The calculated  $\Delta\nu_{1/2}$  versus  $rd$  curve is very similar to Fig. 6.

<sup>†</sup>Supported by the National Science Foundation, GP-9280.

\*Present address: Physics Department, Eastern Oregon College, La Grande, Ore. 97850.

<sup>‡</sup>Present address: National Bureau of Standards, Washington, D. C.

<sup>1</sup>S. Y. Ch'en *et al.* (a) *Phys. Rev.* **144**, 59 (1966); (b) **144**, 66 (1966); (c) **155**, 38 (1967); (d) **156**, 48 (1967).

<sup>2</sup>Cf. F. D. Rossini, *Thermodynamics and Physics of Matter*, (Princeton University Press, Princeton, N. J., 1955).

<sup>3</sup>J. Duperier, L'Universite de Paris, Center d'Orsay, 1966 (report unpublished).

<sup>4</sup>S. Y. Ch'en, E. C. Looi, and R. O. Garrett, *Phys. Rev.* **155**, 38 (1967).

<sup>5</sup>S. Y. Ch'en and R. A. Wilson, *Physica* **27**, 497 (1961).

<sup>6</sup>Behmenburg, *Arkiv Mat. Astron Fysik* (to be published).

<sup>7</sup>E. Lindholm, *Arkiv Mat. Astron Fysik* **32A**, 1 (1945).

<sup>8</sup>J. Fiutak, *Proceedings of the International Conference on Optical Pumping and Spectral Line Shape*, Warsaw, 1968 (to be published).